Application of the Grid-Characteristic Method on Unstructured

Tetrahedral Meshes to the Solution of Direct Problems

in Seismic Exploration of Fractured Layers

V. A. Biryukov, M. V. Muratov, I. B. Petrov, A. V. Sannikov, and A. V. Favorskaya

Moscow Institute of Physics and Technology (State University), Institutskii per. 9, Dolgoprudnyi, Moscow oblast, 141700 Russia e-mail: biryukov.vova@gmail.com, max.muratov@gmail.com, petrov@mipt.ru, donxenapo@gmail.com, aleanera@yandex.ru Received October 22, 2014; in final form, April 28, 2015

Abstract—Seismic responses from fractured geological layers are mathematically simulated by applying the grid-characteristic method on unstructured tetrahedral meshes with the use of high-performance computer systems. The method is intended for computing complicated spatial dynamical processes in complex heterogeneous media and is characterized by exact formulation of contact conditions. As a result, it can be applied to the simulation of seismic exploration problems, including in regions with a large number of inhomogeneities, examples of which are fractured structures. The use of unstructured tetrahedral meshes makes it possible to specify geological cracks of various shapes and spatial orientations. As a result, problems are solved in a formulation maximally close to an actual situation. A cluster of computers is used to improve the accuracy of the computation by optimizing its duration.

DOI: 10.1134/S0965542515100073

Keywords: grid-characteristic method, unstructured tetrahedral meshes, seismic exploration, fractured media, seismic waves, numerical simulation, high-performance computer systems, parallel algorithms.

INTRODUCTION

At present, seismic exploration is a major research method applied before direct drilling [1]. Seismic exploration research is used to determine the structure of rock layers and to identify possible fossil fuel deposits. Numerical experiments make it possible to optimize the interpretation of seismic exploration data, which reduces the costs of oil extraction. In the numerical simulation of such problems, we need to compute seismic wave propagation in rocks with a large number of arbitrarily located inhomogeneities that vary in shape, size, orientation, and physical properties.

To describe such a complex heterogeneous medium most precisely, an optimal approach is to use unstructured tetrahedral meshes, which make it possible to specify inhomogeneities (cracks) of any shape and spatial orientation.

Since the state of a linear elastic solid medium is mathematically simulated using a hyperbolic system of equations [2, 3], an optimal approach is to apply the grid-characteristic method [4–11] with high-order interpolation [12], which allows one to achieve the highest accuracy in the computation of wave propagation.

Examples of using the grid-characteristic method with high-order interpolation on tetrahedral meshes can be found in [11].

The computation of three-dimensional seismic exploration problems requires processing a large amount of data, so high-performance computer systems have to be applied. In this work, we used a cluster of distributed memory computers, on which the developed algorithms were parallelized for optimal use of the resources.

A favorable difference of the approach used in this work from widespread models of effective media [13–16] is that inhomogeneities are directly specified in the integration domain. This approach provides more detailed wave response patterns and allows us to observe qualitatively new effects. Cracks are specified in the form of contact or boundary conditions with the physical properties of the crack-saturating fluid indicated to obtain the most accurate approximation to the model.

Below, we simulate the responses of systems of unidirectional cracks with heights comparable to the length of the incident wavefront. A detailed study of such geological structures is a major problem in modern seismic exploration.

1. MATHEMATICAL MODEL

According to [2], the state of a linear elastic medium is described by the system of equations

$\varrho \partial_t \mathbf{v} = (\nabla \cdot \sigma)^{\mathrm{T}}$, (1) $\partial \sigma = \lambda(\nabla \cdot \mathbf{v})\mathbf{I} + \mu \nabla \otimes \mathbf{v} + (\nabla \otimes \mathbf{v})$. (2)

tensor:

For each of the three systems of the form

we have the exact expression

$\partial_t \mathbf{q} + \mathbf{A}_1 \partial_{\xi_1} \mathbf{q} = 0$ (4)

I $\mathbf{q}(\xi_1,\xi_2,\xi_3,t+\tau) = \sum \mathbf{X}_i \mathbf{q}(\xi_1 - c_i\tau,\xi_2,\xi_3,t)$, (5)

$i=1$

$_t()^{\mathrm{T}}$

Equation (1) is a local equation of motion, in which ϱ is the material density; $\mathbf{v}$ is the velocity of motion; and σ is the Cauchy stress tensor, which is symmetric due to the pair law of shear stresses. Equa□on (2) is derived by differentiating Hooke's law with respect to time. In (2) λ and μ are the Lamé con□tants, which determine the properties of the material.

The following notation is used below: $\partial_t a \equiv \partial a/\partial t$ is the partial derivative of a field a with respect to t; $a \otimes b$ is the tensor product of vectors a and b , $(a \otimes b)^{ij} = a^i b^j$; and $\mathbf{I}$ is the unit tensor of the second rank.

2. NUMERICAL METHOD

System (1), (2) is solved numerically using the grid□haracteristic method on tetrahedral meshes [11]. As a result, correct numerical algorithms can be constructed for computing boundary points and points lying on interfaces between two media with different Lamé constants and (or) different densities.

At every integration time step, we choose three arbitrary directions forming a basis (which ensures the isotropy of the method) and introduce a new coordinate system (ξ_1,ξ_2,ξ_3), in which system (1), (2) can be represented as

$\partial_t \mathbf{q} + \mathbf{A}_1 \partial_{\xi_1} \mathbf{q} + \mathbf{A}_2 \partial_{\xi_2} \mathbf{q} + \mathbf{A}_3 \partial_{\xi_3} \mathbf{q} = 0$, (3) where $\mathbf{q}$ is a vector composed of three velocity components and six components of the symmetric stress

$$\mathbf{q}=\begin{bmatrix}\mathbf{v}\\ \boldsymbol{\sigma}\end{bmatrix}=\{v_1,v_2,v_3,\sigma_{11},\sigma_{22},\sigma_{33},\sigma_{23},\sigma_{13},\sigma_{12}\}^T.$$

where $\mathbf{X}_i$ are matrices expressed in terms of the elements of the matrix $\mathbf{A}_1$, c_i are the eigenvalues of $\mathbf{A}_1$, and τ is the time integration step.

The eigenvalues of all three matrices are expressed in terms of the density and the Lamé constants as follows:

(6)

(7)

$$c_i \in \left\{\sqrt{\frac{\lambda+2\mu}{\varrho}},-\sqrt{\frac{\lambda+2\mu}{\varrho}},\sqrt{\frac{\mu}{\varrho}},-\sqrt{\frac{\mu}{\varrho}},\sqrt{\frac{\mu}{\varrho}},-\sqrt{\frac{\mu}{\varrho}},0,0,0\right\}.$$

In (5) the action of the matrices $\mathbf{X}_i$ on the unknown vector $\mathbf{q}$ can be written as

$$\mathbf{X}_{1,2}\begin{bmatrix}\mathbf{v}\\ \boldsymbol{\sigma}\end{bmatrix}=\frac{1}{2}\begin{bmatrix}(\mathbf{n}\cdot\mathbf{v})\mathbf{n}\mp\frac{1}{c_1\varrho}(\mathbf{N}_{00}\div\sigma\mathbf{I})\mathbf{n},\\ \mp\varrho(\mathbf{n}\cdot\mathbf{v})((c_1-c_3)\mathbf{N}_{00}+c_3\mathbf{I})+\frac{1}{\lambda+2\mu}(\mathbf{N}_{00}\div\sigma)(2\mu\mathbf{N}_{00}+\lambda\mathbf{I})\end{bmatrix}$$

$$\mathbf{X}_{3,4}\begin{bmatrix}\mathbf{v}\\ \sigma\end{bmatrix} = \mathbf{X}_{5,6}\begin{bmatrix}\mathbf{v}\\ \sigma\end{bmatrix} = \frac{1}{2}\begin{bmatrix}\mathbf{v}-(\mathbf{n}\cdot\mathbf{v})\mathbf{n}\mp\frac{1}{c_2\rho}(\sigma\cdot\mathbf{n}-(\mathbf{N}_{00}\div\sigma)\mathbf{n})\\ \mp c_2\rho(\mathbf{n}\otimes\mathbf{v}+\mathbf{v}\otimes\mathbf{n}-2(\mathbf{n}\cdot\mathbf{v})\mathbf{N}_{00})+\mathbf{n}\otimes(\sigma\cdot\mathbf{n})+(\sigma\cdot\mathbf{n})\otimes\mathbf{n}-2(\sigma\div\mathbf{N}_{00})\mathbf{N}_{00}\end{bmatrix}. \qquad (8)$$

The matrices $\mathbf{X}_i$ has the property

$$\sum_{c_i=0}\mathbf{X}_i = \mathbf{I} - \sum_{c_i\neq 0}\mathbf{X}_i.$$

In (6)–(8) $\mathbf{n}$ denotes the unit vector in the direction ξ_1 for the matrix $\mathbf{A}_1$, $\mathbf{N}_{00}$ is the tensor $\mathbf{N}_{00} = \mathbf{n}\otimes\mathbf{n}$, and $\mathbf{A}\div\mathbf{B}$ is a scalar:

$$\mathbf{A}\div\mathbf{B} = \sum_{i=1}^{3}\sum_{j=1}^{3} A_{ij}B_{ij}.$$

Using high-order interpolation in (5) and, in each of the directions ξ_1, ξ_2, and ξ_3, sequentially applying formulas that are similar to (5) and correspond to a system of form (4), we obtain a method for finding the solution at the next time level. The software package applied involves interpolation of the first to fifth orders [12], thereby producing a numerical solution of high accuracy in space. Additionally, the application of the matrices $\mathbf{X}_i$ is implemented with the help of two operators. As a result, the number of interpolations for each point and each direction is reduced from nine to six.

3. BOUNDARY AND CONTACT CORRECTORS

Based on the method applied, the most correct numerical algorithms can be used on the boundaries and interfaces of the integration domain.

Suppose that the boundary condition is written in matrix form as

$\mathbf{D}\mathbf{q}(\xi_1,\xi_2,\xi_3,t+\tau) = \mathbf{d}$, (7) where $\mathbf{q}(\xi_1,\xi_2,\xi_3,t+\tau)$ are the components of the velocity and the stress tensor at the next integration step

at a boundary point. Accordingto(6),eachmatrix$\mathbf{A}_j$ hasthreezeroeigenvalues,threepositive,andthreenegativeones.

To be definite, assume that the characteristics corresponding to the negative eigenvalues of $\mathbf{A}_1$ go beyond the integration domain in the ξ_1 direction.

Then, according to (5), the following sum is calculated at the stage of computing interior points:

$\mathbf{q}^{\text{in}}(\xi_1,\xi_2,\xi_3,t+\tau) = \sum \mathbf{X}_i\mathbf{q}(\xi_1 - c_i\tau,\xi_2,\xi_3,t)$. $c_i \geq 0$

The matrix $\Omega^{*,\text{out}}$ consists of the eigenvectors corresponding to the negative eigenvalues. The corrector at a boundary point is given by the formula

$\mathbf{q}(\xi_1,\xi_2,\xi_3,t+\tau) = \mathbf{F}\mathbf{q}^{\text{in}}(\xi_1,\xi_2,\xi_3,t+\tau) + \Phi\mathbf{d}$, and condition (7) is satisfied to the same order as that of the interpolation.

(8)

The matrix $(\mathbf{D}\Omega^{*,\text{out}})^{-1}$ in formula (8) is found so as to satisfy $(\mathbf{D}\Omega^{*,\text{out}})^{-1}\mathbf{D}\Omega^{*,\text{out}} = \mathbf{I}$,

while the matrices Φ and $\mathbf{F}$ are given by the formulas $\Phi = \Omega^{*,\text{out}}(\mathbf{D}\Omega^{*,\text{out}})^{-1}$,

$\mathbf{F} = \mathbf{I} - \Phi\mathbf{D}$.

In various problems, the boundary conditions are specified as a given external force, a given boundary velocity, mixed boundary conditions, and nonreflecting boundary conditions with outgoing characteris□cs set to zero. In the case of nonreflecting boundary conditions, relation (7) becomes

$\Omega^{\mathrm{out},l/r}\mathbf{q}(t+\tau,\mathbf{r}\ )=\mathbf{0}$ k rp

4. CONDITIONS ON A CRACK

It was found that the most optimal approach in terms of the efficiency of computing actual inhomoge□eities [16] is to specify cracks in the form of contact or boundary conditions. Several crack models spec□fied by various conditions were developed. A crack was assumed to be infinitely thin and filled with a fluid (oil, liquefied gas, or water).

First, we consider two limiting cases of a crack: (i) an open crack filled with a fluid; and (ii) a closed crack, i.e., a crack with edges completely joined together with no fluid in between.

The contact glide condition was used in case (i). This is the mixed contact condition

where V_p and $\mathbf{f}_\tau = 0$ are substituted into the contact conditions for one crack edge with outward normal p, and $-V_p$ and $\mathbf{f}_\tau = 0$, for the other.

In case (ii), we applied the no□lide condition

in in in in

$V_p = (\varrho_a c_{a1}\mathbf{v}_a + \varrho_b c_{b1}\mathbf{v}_b - (\sigma_a - \sigma_b)\cdot\mathbf{p})\cdot\mathbf{p}$, $\varrho_a c_{a1} + \varrho_b c_{b1}$

1 a,in a,in $\mathbf{V} = \varrho c + \varrho c$ $(\varrho_a((\mathbf{p}\cdot\mathbf{v}\ )(c_{1a} - c_{2a})\mathbf{p} + c_{2a}\mathbf{v}\ ) +$

–

$(\mathbf{p}\cdot((\varrho_a c_{1a}\mathbf{v}$

b,in

$)-(\sigma$

a,in

b,in $\Big) \cdot \mathbf{p}))\mathbf{p} \;\Big|.$

$+\varrho_b((\mathbf{p} \cdot \mathbf{v} \;\; \varrho_a (c_{1a} - c_{2a}) + \varrho_b (c_{1b} - c_{2b})$

$) \cdot \mathbf{p} -$

$a \; 2a$

b,in

$b \; 2b \;\;)(c_{1b} - c_{2b})\mathbf{p} + c_{2b}\mathbf{v}$

a,in

$b,\text{in} \; a,\text{in} \; b,\text{in} \;\;) - (\sigma - \sigma$

$-\sigma$ Next, a boundary condition with a given velocity was used for each of the crack edges.

$\varrho \; c + \varrho \; c \;\; a \; 1a \; b \; 1b$

$+\varrho_b c_{1b} \mathbf{v}$

$\Big)$

Actual cracks are combinations of these two model cracks. A crack is closed at some points, while open and filled with a fluid at other points. To simulate such a situation, we developed a crack model with dynamical friction. The computations were performed according to the following algorithm.

Step 1. Compute the case of a completely closed crack to determine the force **f*** at the crack edges. **Step 2.** If **f*** $> k f^*$, then compute the friction

$||||$

τp

$f_p =$

$B,\text{in} \; A,\text{in} \; B,\text{in} \; A,\text{in} \;\; \varrho_A c_{A,1} \varrho_B c_{B,1} ((\mathbf{v} \;\cdot \mathbf{p}) - (\mathbf{v} \;\cdot \mathbf{p})) + \varrho_A c_{A,1} (\sigma \div \mathbf{N}_{00}) + \varrho_B c_{B,1} (\sigma \div \mathbf{N}_{00})$

$1 \; {}_{B,\text{in}\; B,\text{in}} + {}_{\varrho\; c} \; ((\sigma \;\cdot p) - (\sigma$

$B\; B{,}2$

$1 \; {}_{A,\text{in}} \div \mathbf{N}_{00})p) + {}_{\varrho\; c} \; ((\sigma \;\cdot p) - (\sigma$

$A{,}\text{in}$

$\div \mathbf{N}_{00})\mathbf{p}),$

$\varrho c + \varrho c \quad A\; A{,}1\; B\; B{,}1$

$\mathbf{R} = \mathbf{v}^{B,\text{in}} - (\mathbf{v}^{B,\text{in}} \cdot \mathbf{p})\mathbf{p} - \mathbf{v}^{A,\text{in}} + (\mathbf{v}^{A,\text{in}} \cdot \mathbf{p})\mathbf{p} +$

,

$_{A\; A{,}2}\; \mathbf{f} = kf^{\mathbf{R}},$

$^{\tau p}\mathbf{R} \quad \mathbf{f} = f_p\mathbf{p} + \mathbf{f}_\tau.$

Next, the given external force **f** is used as a boundary condition on one edge of the crack and **–f** is used on the other.

Similar computations were performed in the case of a free boundary condition specified on the crack, which approximates an empty (gas-saturated) crack. In this case, the response is the strongest and its structure can be considered in detail.

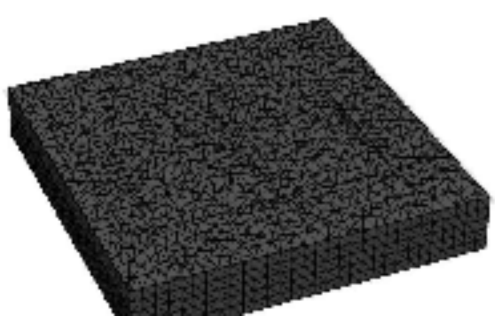

Fig. 1. Example of a tetrahedral unstructured mesh with cracks.

5. UNSTRUCTURED TETRAHEDRAL MESHES

To specify cracks of complex geometry in geological layers, we applied unstructured tetrahedral meshes. They were constructed using a modified version of the open library tetgen. An integration domain with inclusions (cracks) was set first. Then the domain was uniformly filled with tetrahedra of prescribed minimum volume so that the Delaunay criterion was satisfied. Next, the points on the boundaries of the domain and the cracks were optimized for the subsequent computations. The mesh was divided into portions to be used on distributed memory computer systems. Each mesh block consisting of the coordinates of nodes, tetrahedra, triangles, and contact pairs of triangles on opposite sides of the cracks was stored in a binary file and was used by a separate computational node in running the numerical module. Due to the separation of the computational domain between the nodes of the computer system at the initial stage, the amount of data sent out in the course of the computation was minimized, which ensured high efficiency and good scalability of the code. Figure 1 gives an example of a tetrahedral mesh.

6. FEATURES OF THE ROCK MODELS

In the computations, we used rock models based on geometric and physical characteristics maximally similar to actual media.

The integration domain was a box of size 10 × 10 × 3 km. Inhomogeneities (cracks) were placed at a depth of 2 km. The medium parameters were specified as similar to carbonates: the velocities of longitudinal and transverse waves were Vp = 4500 m/s and Vs = 2250 m/s, respectively, and the density was p = 2500 kg/m.

We studied the responses from subvertical cracks of height of about 100 m. The following three models were considered: (1) a single crack, (2) a set (cluster) of unidirectional cracks (Fig. 2), and (3) a set of intersecting cracks (Fig. 3).

The initial perturbation was represented by a plane wave pulse (step) with a wavelength of 150 m.

The results were written in the form of wave patterns of velocity fields in the entire integration domain and in the form of synthetic seismograms from receivers located on the ground surface (daytime surface).

7. RESULTS

Response of a single crack. The 3D simulation of wave propagation in a medium with a single crack was performed. A plane wavefront propa□

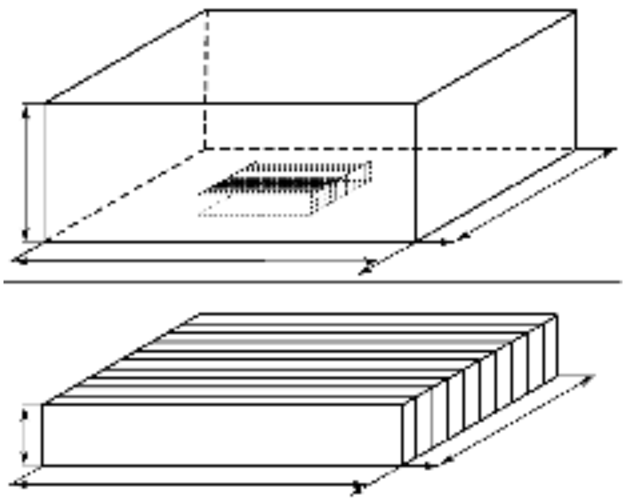

10 km

Y

X

Y 3 km *X*

Fig. 2. Schematic diagram of the system of cracks in the considered problem with geometric sizes indicated.

Fig. 3. Schematic diagram of crack location in a system of intersecting cracks.

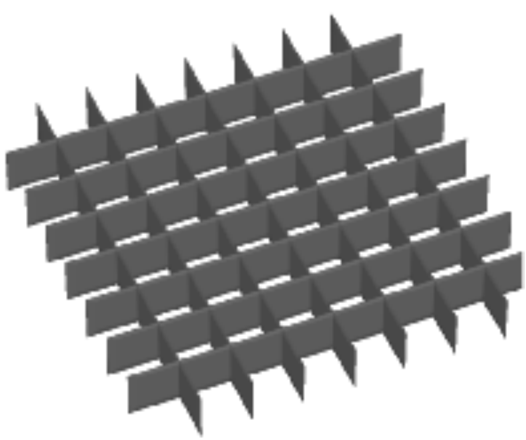

100 m 3 km

10 km

3 km

0.5 0.6 0.7 0.8 0.9 1.0 1.1 1.2 1.3 1.4 1.5 1.6 1.7 1.8

0.5 0.6 0.7 0.8 0.9 1.0 1.1 1.2 1.3 1.4 1.5 1.6 1.7 1.8

(a)

(a)

(b) (c)

Fig. 4. Seismograms of the response of a single liquid-saturated crack.

(b) (c)

Fig. 5. Seismograms of the response of a single empty crack.

. 0.5 0.5

. 0.6 0.6

. 0.7 0.7

. 0.8 0.8

. 0.9 0.9

. 1.0 1.0

. 1.1 1.1

. 1.2 1.2

. 1.3 1.3

. 1.4 1.4

. 1.5 1.5

. 1.6 1.6

. 1.7 1.7

. 1.8 1.8

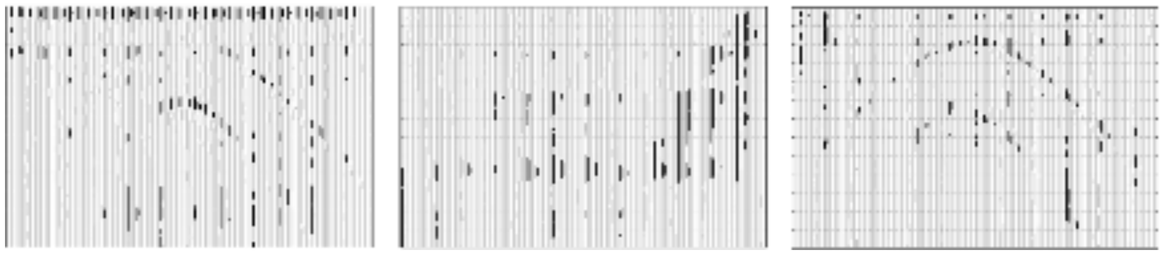

.

. 0.5 0.5

. 0.6 0.6

. 0.7 0.7

. 0.8 0.8

. 0.9 0.9

. 1.0 1.0

. 1.1 1.1

. 1.2 1.2

. 1.3 1.3

. 1.4 1.4

. 1.5 1.5

. 1.6 1.6

. 1.7 1.7

. 1.8 1.8

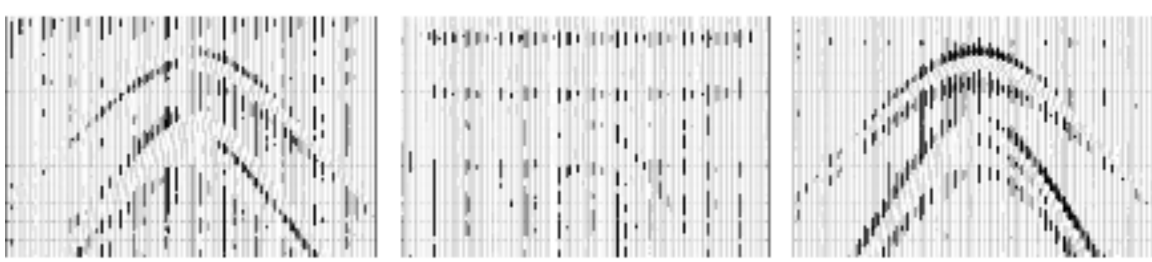

.

(a)

(b)

(c)

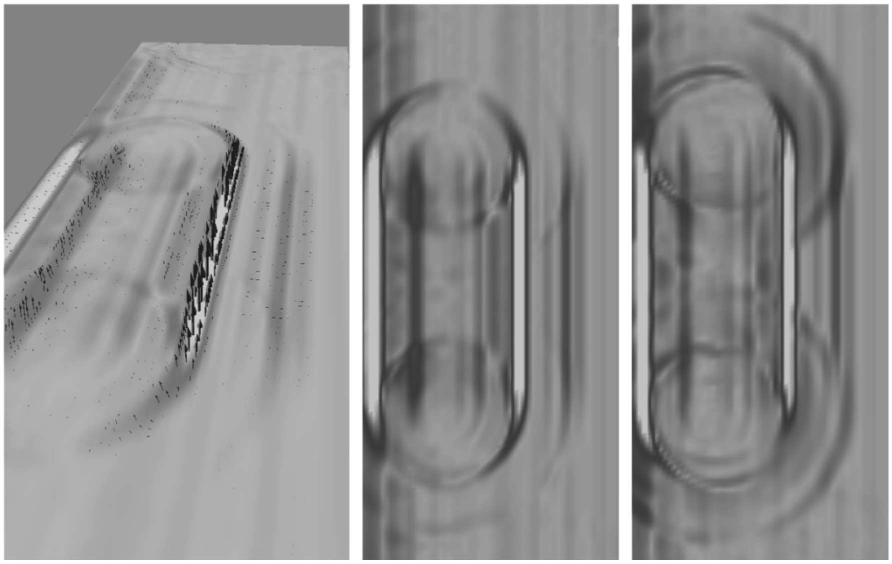

Fig. 6. Two-dimensional wave patterns of the response of a system of unidirectional liquid-saturated cracks (a), (b) in a plane along the crack direction and (c) in a plane across the crack direction.

gated along a crack inclined at a small angle (of about 5°), forming a scattered wave response propagating toward the surface, where it was recorded by seismometers. Seismograms are displayed in Fig. 4. Each vertical line in a seismogram represents a one-dimensional plot of the velocity component obtained at the corresponding seismometer. The figure shows seismograms for three spatial velocity components (a) X, (b) Y, and (c) Z in the case of receivers placed across the plane of the cracks. The response consists of the more intense transverse and less pronounced longitudinal components of the wave scattered by the crack.

A more intense response was obtained in the case of an empty crack (see Fig. 5). Here, the energy of the longitudinal wave prevails in the response.

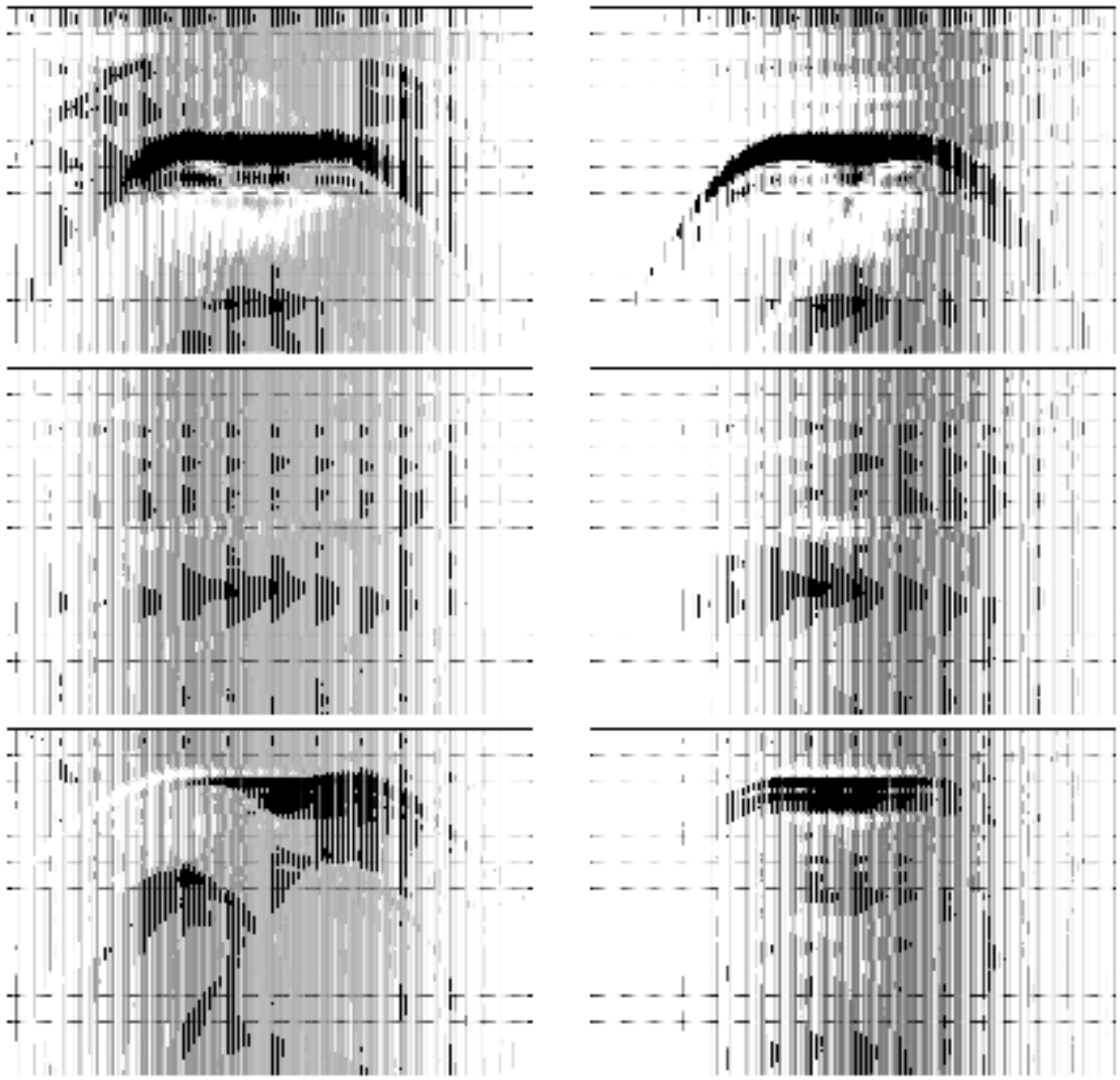

V_x

V_y

V_z

Fig. 7. Seismograms of the wave response of a system of unidirectional liquid-saturated cracks.

It should be noted that the numerical results are similar to those obtained in 2D simulations (see [17– 19]). An issue of special interest is the results obtained from the sensors located along the crack plane, since they cannot be obtained in two-dimensional simulation.

Response of a set of cracks. We investigated the response of a set (cluster) of unidirectional cracks shown schematically in Fig. 2. The cracks were spaced 100 m apart, which was equal to their height. The horizontal sizes of the cluster were 3 × 3 km.

Figure 6 shows the wave patterns of the response in planes parallel and perpendicular to the cracks. The corresponding seismograms of the response are presented in Fig. 7. Figure 8 depicts the two-dimensional area pattern of the response (two-dimensional wave pattern in the plane of the medium surface where the receivers are located) obtained from all sensors on the surface at three different times in the course of arriving the basic energy of the response.

The major portion of the response is represented by a plane wave of multiphase structure propagating upward from the crack cluster. Such a structure is most pronounced in the case of empty cracks (Fig. 9), since the response is stronger.

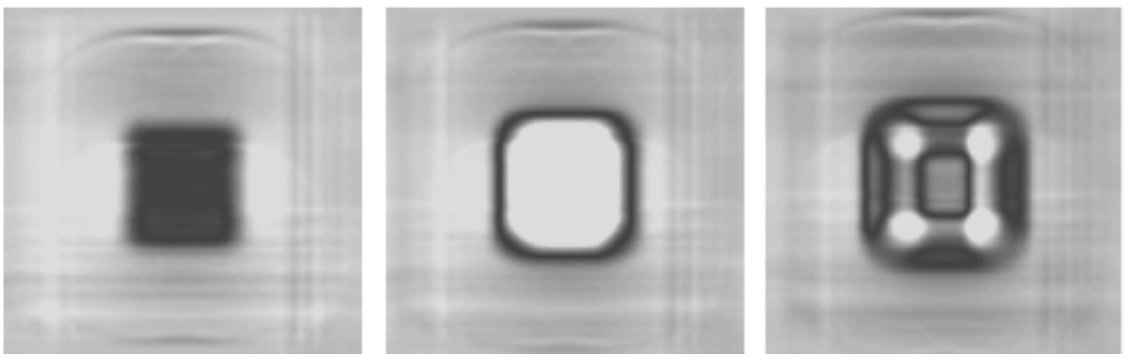

0.5 0.6 0.7 0.8

. V_x 0.9 1.0 1.1 1.2 1.3 1.4 1.5 1.6 1.7 1.8 0.5 0.6 0.7 0.8 0.9 1.0

. V_y 1.1 1.2 1.3 1.4 1.5 1.6 1.7 1.8 0.5 0.6 0.7 0.8 0.9 1.0

. V_z 1.1 1.2 1.3 1.4 1.5 1.6 1.7 1.8

t = 1.18 s t = 1.23 s t = 1.28 s **Fig. 8.** Two-dimensional patterns of the response of liquid-saturated surface cracks (area patterns).

0.5

0.6

0.7

0.8

0.9

1.0

1.1

1.2

1.3

1.4

1.5

1.6

1.7

1.8 0.5

0.6

0.7

0.8

0.9

1.0

1.1

1.2

1.3

1.4

1.5

1.6

1.7

1.8 0.5

0.6 0.7 0.8 0.9 1.0 1.1 1.2 1.3 1.4 1.5 1.6 1.7 1.8

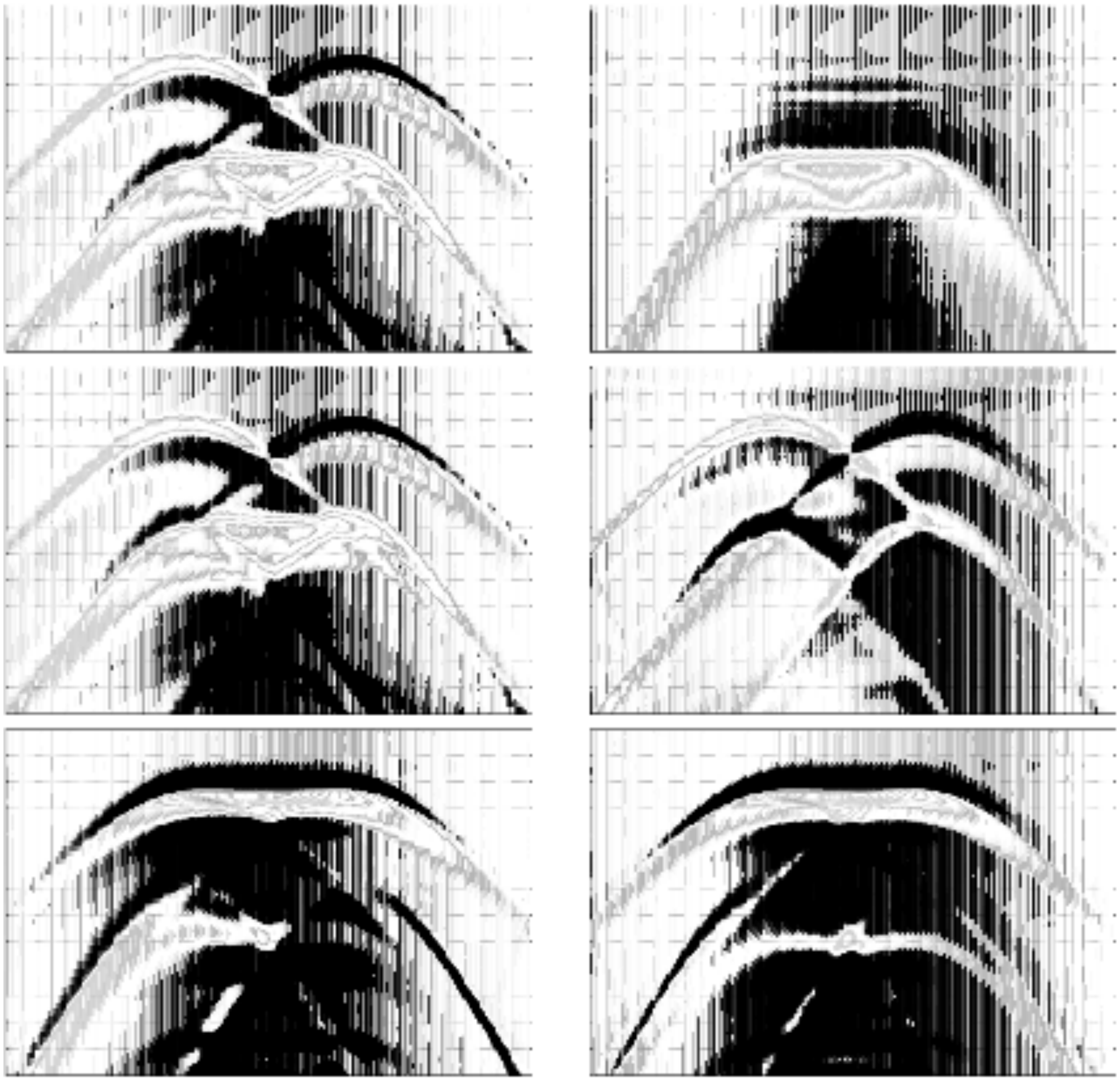

Fig. 9. Seismograms of the wave response of a system of unidirectional empty cracks.

(a) (b)

Fig. 10. Two□mensional wave patterns of the response of a system of cross cracks in (a) vertical plane and (b) horizontal plane.

Response of a system of cross cracks. We studied the response of a system of cross cracks (see Fig. 3). Figure 10 presents the wave patterns of the response after the flat wavefront passed through the system. Specifically, one of the vertical planes in which the wavefront propagates is shown in Fig. 10a, while the pattern in a horizontal plane intersecting the crack is displayed in Fig. 10b.

The results of this work were obtained using the computational resources of the

Multifunctional Computing Center of the National Research Center "Kurchatov Institute" (http://computing.kiae.ru/).

ACKNOWLEDGMENTS This work was supported by the Russian Science Foundation, grant no. 14-11-00263.

REFERENCES

1. R. E. Sheriff and L. P. Geldart, *Exploration Seismology* (Cambridge Univ. Press, Cambridge, 1982; Mir, Moscow, 1987).

2. W. Nowacki, *Thermoelasticity* (Pergamon, Oxford, 1962; Mir, Moscow, 1975).

3. V. I. Kondaurov and V. E. Fortov, *Fundamentals of Thermal Mechanics of Condensed Media* (Mosk. Fiz.-Tekh. Inst., Moscow, 2002) [in Russian].

4. K. M. Magomedov and A. S. Kholodov, *Grid-Characteristic Numerical Methods* (Nauka, Moscow, 1988) [in Russian].

5. A. G. Kulikovskii, N. V. Pogorelov, and A. Yu. Semenov, *Mathematical Aspects of Numerical Solution of Hyperbolic Systems* (Fizmatlit, Moscow, 2001; Chapman and Hall/CRC, London, 2001).

6. I. B. Petrov and A. S. Kholodov, "Numerical study of some dynamic problems of the mechanics of a deformable rigid body by the mesh-characteristic method," USSR Comput. Math. Math. Phys. **24** (3), 61–73 (1984).

7. A. S. Kholodov, "Numerical methods for solving hyperbolic equations and systems," in *Encyclopedia of Low-Temperature Plasmas* (Yanus-K, Moscow, 2008), Vol. VII-1, Part 2, pp. 141–174 [in Russian].

8. V. D. Ivanov, V. I. Kondaurov, I. B. Petrov, and A. S. Kholodov, "Computation of dynamic deformation and fracture of elastoplastic bodies by grid-characteristic methods," Mat. Model. **2** (1), 11–29 (1990).

9. I. B. Petrov and A. S. Kholodov, "Regularization of discontinuous numerical solutions of equations of hyperbolic type," USSR Comput. Math. Math. Phys. **24** (4), 128–138 (1984).

10. I. B. Petrov, A. G. Tormasov, and A. S. Kholodov, "On the use of hybrid grid-characteristic schemes for the numerical solution of three-dimensional problems in the dynamics of a deformable solid," USSR Comput. Math. Math. Phys. **30** (4), 191–196 (1990).

11. A. V. Favorskaya, I. B. Petrov, I. E. Kvasov, and A. V. Sannikov, “Grid□haracteristic method using high□rder interpolation on tetrahedral hierarchical meshes with a multiple time step,” Math. Model. Comput. Simul. **5** (5), 409–415 (2013).

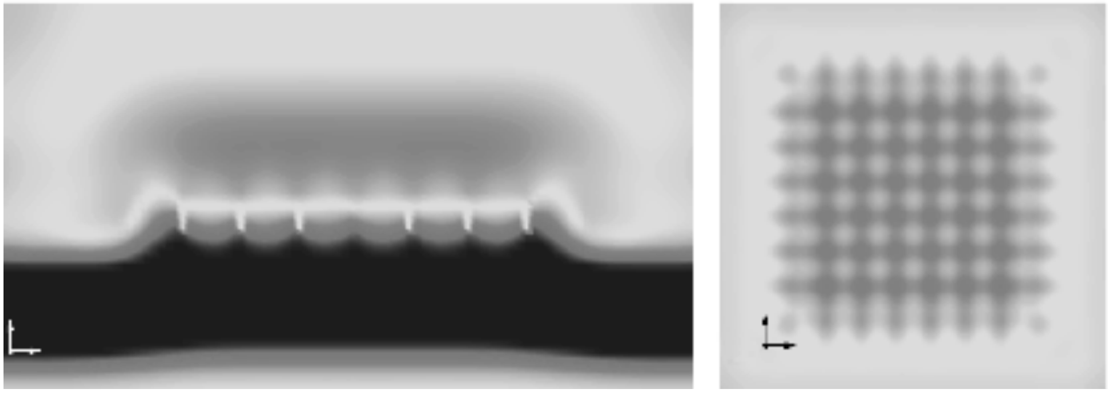

Y Z X

12. I. B. Petrov and A. V. Favorskaya, “Library of high□rder interpolation methods on unstructured triangular and tetrahedral meshes,” Zh. Inf. Tekhnol., No. 9, 30–32 (2011).

13. C.J.HsuandM.Schoenberg,“Elasticwavesthroughasimulatedfracturedmedium,”Geophysics**58**(7),964– 977 (1993).

14. M. E. Willis, at al., “Spatial orientation and distribution of reservoir fractures from scattered seismic energy,” Geophysics **71** (5), 43–51 (2006).

15. L.A.MolotkovandA.V.Bakulin,“Effectivemodelofalayeredelasticporousmedium,”Dokl.Akad.Nauk**372** (1), 108–112 (2000).

16. E. A. Kozlov, *Medium Models in Exploration Seismology* (Gers, Tver, 2006) [in Russian].

17. V. B. Levyant, I. B. Petrov, and I. E. Kvasov, “Numerical simulation of wave response of subvertical macrofrac□tures, possible fluid□onducting channels,” Tekhnol. Seismorazvedki, No. 4, 4–29 (2011).

18. V. B. Levyant, I. B. Petrov, and M. V. Muratov, “Numerical simulation of wave responses from subvertical mac□ofractures system,” Tekhnol. Seismorazvedki, No. 1, 5–21 (2012).

19. V. B. Levyant, I. B. Petrov, M. V. Muratov, and S. A. Byko, “Stability analysis of the

formation of a front of con□erted waves from a zone of macrofractures," Tekhnol. Seismorazvedki, No. 1, 32–45 (2013).

Translated by I. Ruzanova